ACADEMIA ROMÂNĂ
Revue Roumaine de Chimie
http://web.icf.ro/rrch/

Rev. Roum. Chim.,
2017, *62*(1), 5-14

MECHANISM OF (E)-2-(4-METHOXYBENZYLIDENE)HYDRAZINECARBOXAMIDE CYCLIZATION: DENSITY FUNCTIONAL THEORY APPROACH

Abdulfatai Adabara SIAKA,[a*] Adamu UZAIRU,[b] Sulaiman Ola IDRIS[b] and Hamza ABBAH[b]

[a] Department of Applied Chemistry Federal University Dutsin-ma Katsina Nigeria
[b] Department of Chemistry, Ahmadu Bello University, Zaria Kaduna Nigeria

Received January 28, 2016

The reaction between 4-methoxybenzadehyde and the semicarbazide was investigated using semi-empirical/Austin model (AM1) and Density functional theory (DFT) [RB3LYP/6-31G(d)] calculations in SPARTAN,2009 program suit. The two reaction pathways were found to consist several elementary steps comprising intermediate and transition states. The cyclization of (E)-2-(4-methoxybenzylidene)hydrazinecarboxamide was found via two routes. From the kinetic data it was observed that the consecutive step between second and third intermediates with rate constant value of 1.64 s^{-1} is the rate determining step of the reaction mechanism for the first path way. But for the alternative reaction pathway, the step between the third and fourth intermediates with rate constant value of $1.44 \cdot 10^{-4}$ s^{-1} is the rate determining step. Though two cyclization routes were all endothermic, cyclization route 2 was more endothermic. Hence, the reaction pathway (route 1) was most stable favorable as shown in the potential energy curve. This is also collaborated by the thermodynamic data for the two reaction pathways.

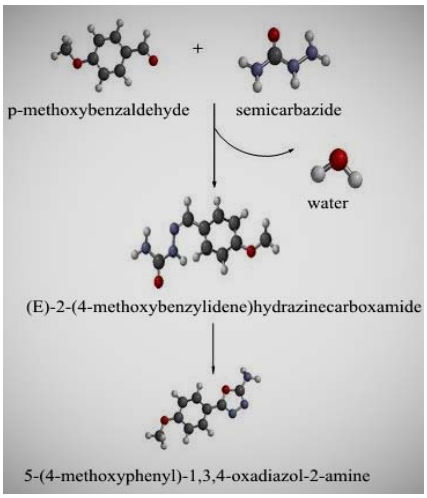

INTRODUCTION

Semicarbazones are derivatives of imines formed from the reaction of an aldehyde or ketone with the terminal $-NH_2$ group of semicarbazide, which behaves very similarly to primary amines. Semicarbazide, the raw material, from which semicarbazones are formed have been known to have biological activity against many of the most common species of bacteria.[1] Oxadiazoles belong to a group of heterocyclic that have been attracting attention for last two decades due to their wide range of biological interactions. The 1,3,4-oxadiazole ring system has been identified as the main core of many bioactive molecules. Compounds containing these aromatic five-membered heterocycles have been shown to exert anti-inflammatory,[2] antimicrobial,[3] anti-convulsant,[4] and hypoglycaemic[5] activities. In addition, 2,5-disubstituted-1,3,4-oxadiazoles are proposed to have potential agrochemical use[6] due to their wide spectrum of insecticidal[7] and acaricidal[8] properties attained by interfering with insect's chitin biosynthesis.[9] This class of materials also has gained the worth of modern applications such as scintillators, fluorescence and photographic materials.

Invariably, Semicarbazones themselves are of much interest due to a wide spectrum of anti-fungal and anti-bacterial activities.[10] Recent review

* Corresponding author: fatsaadaby@gmail.com

on bioactivity of semicarbazones showed that they exhibit anti-convulsant, anti-tubercular,[11] anti-oxidant, anti-microbial, analgesic, anti-pyretic and anti-inflammatory activities.

Many natural and synthetic compounds are capable of affecting selectively specific organs and tissues within a biological system. In spite the importance of this class of compound, literature is very scanty about empirical information on their reaction, while theoretical information seems unavailable to the best of my knowledge. Hence, this study is aimed at providing theoretical information on (E)-2-(4-methoxybenzylidene)hydrazinecarboxamide (semicarbazone) formation and its cyclization reaction to form 5-(4-methoxyphenyl)-1,3,4-oxadiazol-2-amine. The cyclization outline of the studied semicarbazone is presented in Fig. 1 below.

COMPUTATIONAL METHODS

The geometries of the reactants, transition states, intermediate and products were optimized using Molecular mechanics to remove strain energies. This was followed by semi empirical optimizations at AM1 theory level. Finally, density functional theory (DFT) Becke's three parameter nonlocal exchange functional with the nonlocal correlation functional of Lee, Yang, Parr (B3LYP) with 6-31G(d) basis set calculations was employed. [12] Furthermore, heat of formation was calculated for all the stationary points using thermochemical recipe at T_1 theory level.[13] For equilibrium geometries and transition states, the nature of the critical points was confirmed by an analytic frequency computation. All the transition states have imaginary frequencies. Intrinsic reaction coordinate calculations were carried out to confirm that the transition states connect to the right minima. All the energy parameters of the reaction mechanisms I and II are calculated using the expressions below as reported in.[14]

$$\Delta G^{\#}_{(298.15K)} = \Delta H - T\Delta S^{\#} \quad (1)$$

$$k_{(298.15K)} = \frac{k_B T}{hC^{\circ}} e^{\Delta S^{\#}/R_e - \Delta H^{\#}/RT} \quad (2)$$

$$K_{(298.15K)} = e^{-\Delta G^{\circ}/RT} \quad (3)$$

$$A = \frac{e^2 k_B T}{hc^{\circ}} e^{\frac{\Delta S^{\#}}{R}}, \text{ for bimolecular} \quad (4)$$

$$A = \frac{e k_B T}{h} e^{\frac{\Delta S^{\#}}{R}}, \text{ for uni-molecular} \quad (5)$$

where $\Delta G^{\#}$, $\Delta H^{\#}$ and $\Delta S^{\#}$ stand for Gibbs energy change, enthalpy change and entropy change for reaction between reactant(s) and a transition state.

RESULT AND DISCUSSION

Semicarbazones formation and cyclization mechanism and rate law

The detailed reaction scheme for the formation and subsequent cyclization is as presented in Fig. 2 below.

Reaction enthalpy, entropy, Gibbs energy (for consecutive steps), and activation enthalpy, entropy of activation including Gibbs energy of activation (for transition steps) of the formation of 5-(4-methoxyphenyl)-1,3,4-oxadiazol-2-amine were evaluated, and the results were presented in Table 1. Collision frequency, activation energy, rate constant and equilibrium constant values of the 4-methoxybenzaldehyde–hydrazinecarboxamide reaction system were presented in Table 2. In these Tables, A represented 4-methoxybenzaldehyde, B was hydrazinecarboxamide, TS1 was transition state 1, INT1 was intermediate 1, TS2 was transition state 2, INT2 was intermediate 2, TS3 was transition state 3, INT3 was intermediate 3, TS4 was transition state 4, INT4 was intermediate 4, TS5 was transition state 5, while P1 and P2 were minor and major products respectively.

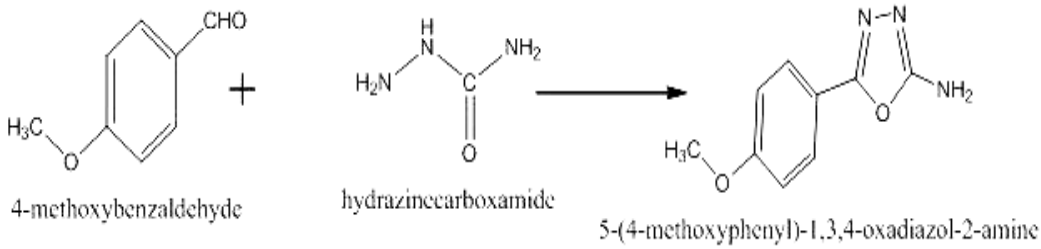

Fig. 1 – Semicarbazone cyclization outline.

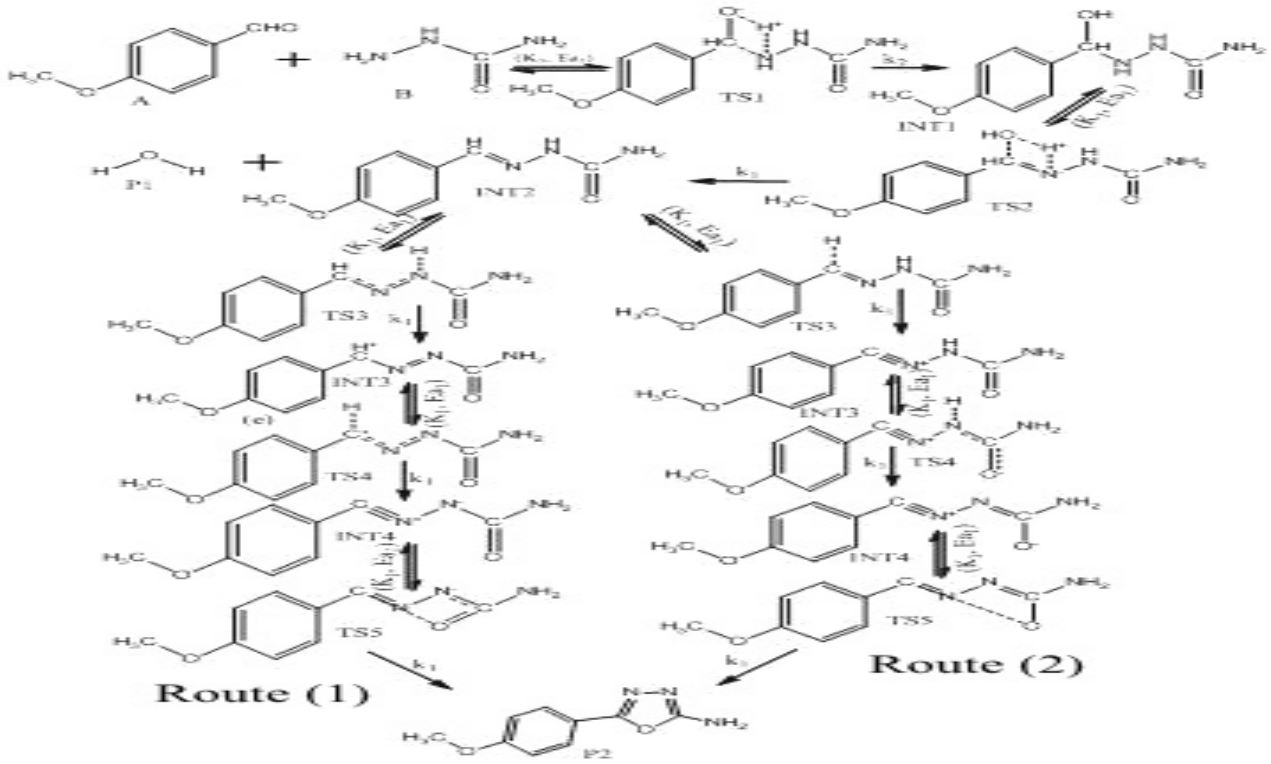

Fig. 2 – General reaction scheme for electrocyclization of semicarbazone.

Table 1

DFT B3LYP (6-311+G**) Calculated Thermodynamics Parameters
for p-methoxybenzaldehyde and hydrazinecarboxamide cyclization reaction at 298.15 K route 1

Steps	**($Jmol^{-1}K^{-1}$)**	**($kJmol^{-1}$)**	**($kJmol^{-1}$)**	**($Jmol^{-1}K^{-1}$)**	**($kJmol^{-1}$)**	**($kJmol^{-1}$)**
A + BTS1	-195.36	-38.16	+20.09			
A+BINT1				-193.36	-29.83	+27
INT1TS2	-7.04	+2.83	+4.93			
INT1INT2+P1				+161.95	+1.51	-46.77
INT2 TS3	-54.94	+32.59	+48.97			
INT2INT3				-53.34	+854.96*	+16.76 *
INT3 TS4	-1.82	-22.49	-21.95			
INT3 INT4				-6.59	???	???
INT4 TS5	+17.69	-25.68	-20.41			
INT4 P2				-13.87	-129.04	-124.90

Table 2

DFT B3LYP (6-311+G**) Calculated kinetic parameters
for p-methoxybenzaldehyde and hydrazinecarboxamide cyclization reaction at 298.15 K route 1

Steps	**A**	**k_2 ($dm^3mol^{-1}s^{-1}$)**	**K_2**	**k_1 (s^{-1})**	**K_1**
A + BTS1	2.87 $dm^3mol^{-1}s^{-1}$		3.03		
A+BINT1		1.88			
INT1TS2	7.24s^{-1}				1.37
INT1INT2+P1				3.66s^{-1}	
INT2 TS3	2.28 s^{-1}				2.64
INT2INT3				1.64	
INT3 TS4	1.36 s^{-1}				7.00
INT3 INT4				4.34	
INT4 TS5	2.01 s^{-1}				3.76
INT4 P2				2.33	

The formation of transition state TSI is calculated to be exothermic (from enthalpy of activation value) but non-spontaneous from Gibbs' energy of activation value presented in the Table 1 above. The step has excess energy of about 18 kJ/mol which is far below the energy barrier for the step, hence external energy source is required for the step to be initiated. Pre-exponential factor and equilibrium constant values for the bimolecular transition step are low, indicating that some adjustment (in term of energy) is necessary for the equilibrium to be shifted forward. The unimolecular transition step is computed to be endothermic and non-spontaneous with a very high energy barrier. This step has an energy demand of about 196 kJ/mol for successful reaction. But this step is characterized with high collision factor and equilibrium values compared to the unimolecular transition step. The first consecutive step (bimolecular) has high exothermicity value compared to non-spontaneity value, with excess energy of 2 kJ/mol, suggesting the thermodynamic feasibility of the step. The bimolecular step is also calculated to be the rate determining step as seen in the Table below. The second unimolecular consecutive step is computed to be slightly endothermic but hugely spontaneous with an excess energy of over 40 kJ/mol.

The step connecting the second intermediate with the third intermediate was found to be highly demanding energetically as it is associated with positive enthalpy and Gibbs energy of activation; in addition the consecutive step is endergonic and endothermic. However both the transition and consecutive steps were found to be associated with entropy decrease. The next dehydrogenation step was found to be thermodynamically feasible as the step was computed to be exergonic and exothermic having low Gibbs energy, enthalpy and entropy of activation. Similar trend was observed for transition step connecting the fourth intermediate with the final product formation step as presented in Table 1 above. Among all the steps in the cyclization mechanism, the second consecutive step between the second intermediate and third intermediate through the third transition state was found to be rate determining step, while the transition step between the second intermediate and third transition state was also found to have the least equilibrium constant value. The kinetic values are presented in the Table 2 above.

Table 3

DFT B3LYP (6-311+G**) Calculated Thermodynamics Parameters
for p-methoxybenzaldehyde and hydrazinecarboxamide cyclization reaction at 298.15 K route 2

Steps	**($Jmol^{-1}K^{-1}$)**	**($kJmol^{-1}$)**	**($kJmol^{-1}$)**	**($Jmol^{-1}K^{-1}$)**	**($kJmol^{-1}$)**	**($kJmol^{-1}$)**
A + BTS1	-195.36	-38.16	+20.09			
A+BINT1				-193.36	-29.83	+27
INT1TS2	-7.04	+2.83	+4.93			
INT1INT2+P1				+161.95	+1.51	-46.77
INT2 TS3	-56.09	-19.26	-2.54			
INT2INT3				-59.93	+191.83	+209.70
INT3 TS4	+23.91	+102.08	+94.95			
INT3 INT4				+0.64	-25.73	-25.92
INT4 TS5	-2.95	-103.16	-102.28			
INT4 P2				-14.51	-103.31	-98.98

Table 4

DFT B3LYP (6-311+G**) Calculated kinetic parameters
for p-methoxybenzaldehyde and hydrazinecarboxamide cyclization reaction at 298.15 K route 2

Steps	**A**	**k_2 ($dm^3mol^{-1}s^{-1}$)**	**K_2**	**k_1 (s^{-1})**	**K_1**
A + BTS1	2.87 $dm^3mol^{-1}s^{-1}$		3.03		
A+BINT1		1.88			
INT1TS2	7.24s^{-1}				1.37
INT1INT2+P1				3.66	
INT2 TS3	1.98 s^{-1}				2.78
INT2INT3				1.73	
INT3 TS4	3.00 s^{-1}				0
INT3 INT4				1.44	
INT4 TS5	1.18 s^{-1}				8.30
INT4 P2				5.15	

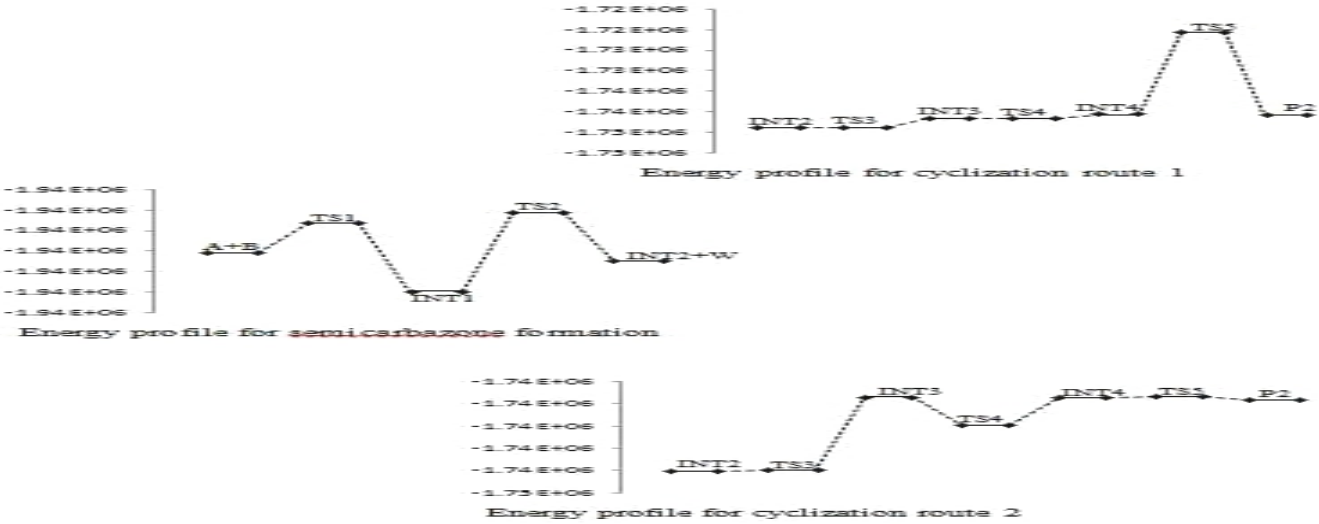

Fig. 3 – Diagram of relative electronic energies along the reaction channel between p-methoxybenzaldehyde and hydrazinecarboxamide cyclization system.

The reaction was found to occur via two endothermic routes among which route one was observed to be thermodynamically more feasible than the route two according to the potential energy profile of the reaction in Fig. 3 below. Profile of p-methoxybenzaldehyde reaction with hydrazinecarboxamide was obtained by plotting electronic energy (potential energy) calculated at DFT theory level for all the stationary points against the reaction coordinates. The profile is presented in Fig. 3 (potential energy) where (A+B), TS1, INT1, TS2, (INT2+P1), TS3, INT3, TS4, INT4, TS5 and P2 on the saddle points are the reactants, transition state 1, intermediate 1, transition state 2, intermediate 2 including the minor product, transition state 3, intermediate 3, transition state 4, intermediate 4, transition state 5 and the major product respectively (Fig. 3).

Geometry optimization of p-methoxybenzaldehyde and hydrazinecarboxamide cyclization system

From Table 5, C2–C8 bond was seen to have progressively and marginally increased through the transformation. Similar pattern (but higher margin) of bond extension was observed on C8–O1 as the process progresses via first transition state, intermediate and second transition state. From first transition state to intermediate the partial bond initiated between C8 and N1 at the transition state was found to have been actually established at the intermediate stage. Again similar partial was seen to be initiated at the second transition state leading to double bond formation in the final product. Consequently the C8–N1 bond contracted considerably from TS1 through INT to TS2.

Bond angle C2C8O1 was found to have decreased continuously from TS1 to TS2 as the oxygen prepares to leave the molecule in the final product. On the other hand the bond formation initiated at the first transition state and maintained through the transformation lead to increased C2C8O1 bond angle. Competing bond formation and bond cleavage characters were observed on C2C8H10 with the bond formation dominating as the bond angle, which decreased from TS1 to INT and later increased as the process continued from INT to TS2. Similar but slight bond formation dominance was observed on O1C8H9 as the transformation proceeded from TS1 to TS2 through INT. Throughout the process the persistent bond formation character between O1–H2 showed dominance over the bond cleavage character as the C8O1H2 bond angle experienced increase from TS1 to TS2. However bond fission character between C8–O2 seemed to have taken prominence as the process progressed to TS2 from INT leading to constriction in N1C8O1 bond angle. This geometry information is presented in the Table 6 above.

As presented in Fig. 4 below, the HOMO–LUMO for p-methoxybenzaldehyde and hydrazinecarboxamide cyclization system showed energy gap of –4.99 eV for p-methoxybenzaldehyde (particularly on C8 of the carbonyl group). This is larger than the HOMO–LUMO energy gap (E = –3.00 eV) on N1 for hydrazincarboxamide, according to Fukui's frontier orbital theory. Again these HOMO–LUMO energy gap values suggested

that while the hydrazinecarboxamide would behave as a better electron donor, the p-methoxybenzaldehyde would be the electron acceptor. Furthermore, the HOMO orbital was seen to be highly situated on C8 while the LUMO density was located on N1 of the first intermediate molecule with HOMO–LUMO energy gap (E = –5.73 eV). Similar observation showed that the second intermediate has HOMO–LUMO energy gap of –4.44 eV, while the third and fourth intermediates have energy gaps of –5.86 eV and –4.55 eV respectively.

A closer look at the charge distributions shows that partial charges are highly concentrated around C1, C2 and C8 and O2 on p- methoxybenzaldehyde, and N1, N3 and H1 on semicarbazide molecules, but with varying values of exposed area. As a result of variation in the exposed area C8, O2, N1 and H1 were able to engage in reaction leading to formation of first transition state (TS1) owing largely to less steric effect consequent of large exposed surface. This observation is presented in the Table 7 below.

Table 5

Variations in bond length during transformation through TS1, INT and TS2 for p-methoxybenzaldehyde and hydrazinecarboxamide cyclization system

TS1	Bond Length ()	INT	Bond Length ()	TS2	Bond Length ()
C2,C8	1.516	C2,C8	1.514	C2,C8	1.444
C8,O1	1.344	C8,O1	1.410	C8,O2	2.349
C8,N1	1.633	C8,N1	1.486	C8,N1	1.325
N1,H10	1.024	N1,H11	1.025	N1,H11	1.046
N1,N2	1.413	N1,N2	1.419	N1,N2	1.406
O1,H2	1.397	O2,H9	0.972	O2,H9	0.972

Table 6

Variations in bond Angles during transformation through TS1, INT and TS2 for p-methoxybenzaldehyde and hydrazinecarboxamide cyclization system

TS1		**INT**		**TS2**	
C2C8O1	118.12 º	C2C9O2	108.94	C2C8O2	89.07
C2C8N1	108.09 º	C2C8N1	115.78 º	C2C8N1	125.80 º
C2C8H9	111.29 º	C2C8H10	109.11 º	C2C8H10	117.92 º
N1C8O1	94.06 º	N1C8O2	105.87 º	N1C8O2	75.10 º
O1C8H9	117.42 º	O2C8H10	111.93 º	O2C8H10	119.82 º
C8O1H2	77.22 º	C8O1H9	105.52 º	C8O1H9	145.39 º
C8N1H10	117.50 º	C8N1H11	108.38 º	C8N1H11	109.74 º
C8N1N2	117.44 º	C8N1N2	111.97	C8N1N2	117.30 º

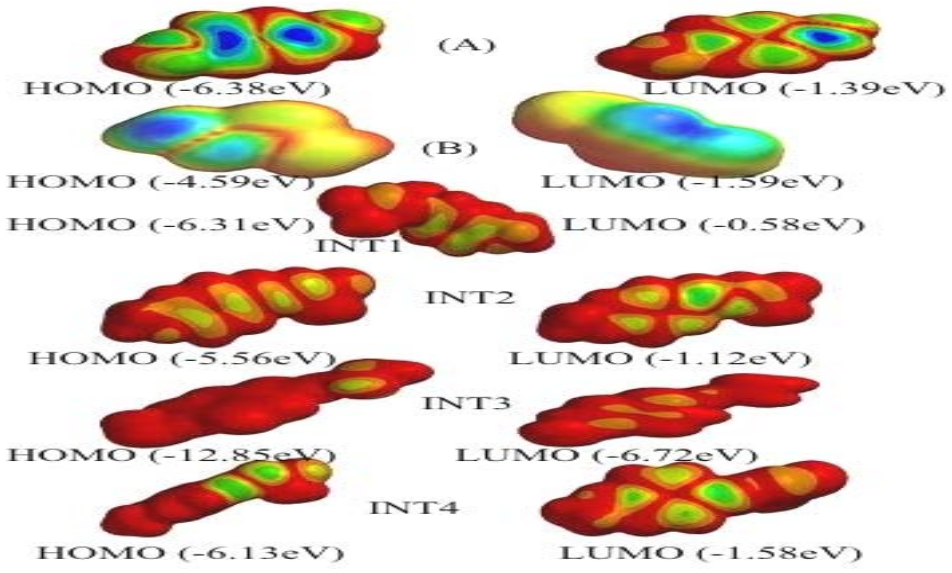

Fig. 4 – HOMO-LUMO energy for p-methoxybenzaldehyde-hydrazinecarboxamide cyclization system.

Table 7

Atomic charge distribution and exposed area (Å^2) for p-methoxybenzaldehyde (A), semicarbazide (B) and first intermediate (INT1)

	A		**B**		**INT1**	
Atom	Mulliken Charge	Exposed Area(Å^2)	Mulliken Charge	Exposed Area(Å^2)	Mulliken Charge	Exposed Area(Å^2)
C3	-0.17	13.72				
C6	-0.19	12.15				
C5	-0.19	12.96				
C7	-0.16	12.94				
C8	+0.19	17.52			+0.51	7.51
O2	-0.42	14.75			-0.62	11.51
H8					+0.31	7.72
N1			-0.57	10.80	-0.45	4.41
N2			-0.50	5.50	-0.48	4.91
C1			+0.68	15.98		
N3			-0.755	7.60	-0.75	7.32

In the Table below, partial charge distributions are most prominent on C8, N1, O2 and H8. The interaction between C8 and N1 leading to formation of C=N is more favored charge wise than steric effect (less exposed surface), while the interaction between O2 and H8 leading to formation of leaving group in second transition state (TS2) is favored both in charge distribution and exposed surface area. Also partial withdrawal of charges towards O2 from C8 is observed by partial C8–O2 bond cleavage with attendant increased C8 exposed surface. Similar charge withdrawal towards N1 with increased surface area is also observed between N1 and H8.

From the charge distribution and exposed surface area presented in Table 8 below, interactions between C8 and H9 (partial bond cleavage) and C8 and N1 (partial bond formation) in the third transition state (TS3) are highly favored by exposed surface area than by charge distribution. The interaction eventually leads to increased exposed surface area around C8.

Though interaction in form of partial bond cleavage between N2 and H10 by virtue of charge distribution leading to fourth transition state (TS4) is suggested, it is not well encouraged by exposed surface area (less). Meanwhile high charge distribution and large exposed area encourage partial interaction between C9 and O2 with somewhat increase in exposed area for O2 as presented in Table 5 above. Though C8 is well exposed for interaction, it is disadvantaged charge wise.

As shown in Table 9 below, exposed surface area and charge distribution highly favor interactions within the intermediate (INT4). Interaction between C8 and N1 leading to partial bond cleavage the atoms is well encouraged with less steric effect. Similar trend is also observed between C11 and O2 leading to partial bond formation between the two atoms in the fifth transition state (TS5).

Form the charge distribution presented above, interactions within the third intermediate (INT3b) as suggested by the alternative mechanism is not feasible, and the possibility is further complicated by small exposed surface area. Though partial interactions between C8 and H9 and N1 and N2, the worst hit is the N1 and N2, which is not favored by both charge distribution and steric effect.

Table 8

Atomic charge distribution and exposed area (Å^2) for INT2, INT3a and INT4a first route

	INT2		**INT3**		**INT4**	
Atom	Mulliken Charge	Exposed Area(Å^2)	Mulliken Charge	Exposed Area(Å^2)	Mulliken Charge	Exposed Area(Å^2)
C2	+0.38	5.72	+0.125	5.61	+0.13	5.64
C8	+0.024	15.34	+0.393	20.41	+0.17	20.23
N1	-0.254	7.501	-0.28	5.51	-0.09	4.72
N2	-0.465	4.177	-0.4.9	5.25	-0.42	10.29
H9	+0.116	5.479			+0.51	7.51
N3	-0.759	4.18	-0.749	7.00	-0.62	11.51
C11					+0.68	17.12

Table 9

Atomic charge distribution and exposed area (Å^2) for INT2, INT3b and INT4b second route

	INT2		**INT3b**		**INT4b**	
Atom	Mulliken Charge	Exposed Area(Å^2)	Mulliken Charge	Exposed Area(Å^2)	Mulliken Charge	Exposed Area(Å^2)
C2	+0.38	5.72	+0.11	5.69	+0.14	5.59
C8	+0.024	15.34	+0.09	15.34	+0.15	20.08
N1	-0.254	7.501	-0.18	7.81	-0.09	4.68
N2	-0.465	4.177	-0.23	9.09	-0.42	10.21
H2			+0.21	5.41		
N3	-0.759	4.18	-0.74	6.89		
C9			+0.72	16.98	+0.67	17.13

Again in this intermediate, interaction between C8 and N1 is well encouraged by charge distribution but disadvantaged by exposed surface area especially for N1. N2 and C9 interaction is both favored by charge distribution and exposed area. Also, C8 and O2 interaction is highly favored by exposed surface area but disadvantaged by charge distribution as presented in the Table above. Hence, the mechanism represented by the species above cannot be possible.

The cyclization and rate law

The elementary steps and the rate law of the cyclization mechanism are as shown below;

$$A + B \underset{k'_{-2}}{\overset{k'_2}{\rightleftharpoons}} AB^{\#}$$

$$AB^{\#} \xrightarrow{k_1} C$$

$$C \underset{k'_{-1}}{\overset{k'_1}{\rightleftharpoons}} C^{\#}$$

$$C^{\#} \xrightarrow{k_1} D$$

$$D \underset{k'_{-1'}}{\overset{k'_{1'}}{\rightleftharpoons}} D^{\#}$$

$$D^{\#} \xrightarrow{k_{1'}} E$$

$$E \underset{k'_{-1''}}{\overset{k'_{1''}}{\rightleftharpoons}} E^{\#}$$

$$E^{\#} \xrightarrow{k_{1''}} F$$

$$F \underset{k'_{-1'''}}{\overset{k'_{1'''}}{\rightleftharpoons}} F^{\#}$$

$$F^{\#} \xrightarrow{k_{1'''}} P$$

The reaction rate law can be written as thus;

$$\frac{d[P]}{dt} = k'_{1'''}[F^{\#}] \quad (1)$$

$$\frac{d[F^{\#}]}{dt} = k'_{1'''}[F] - k'_{-1'''}[F^{\#}] - k_{1'''}[F^{\#}] \quad (2)$$

$$\frac{d[F]}{dt} = k_{1''}[E^{\#}] + k'_{-1'''}[F^{\#}] - k'_{1'''}[F] \quad (3)$$

$$\frac{d[E^{\#}]}{dt} = -k_{1''}[E^{\#}] - k'_{-1''}[E^{\#}] + k'_{1''}[E] \quad (4)$$

$$\frac{d[E]}{dt} = -k_{1'}[D^{\#}] + k'_{-1''}[E^{\#}] - k'_{1''}[E] \quad (5)$$

$$\frac{d[D^{\#}]}{dt} = -k_{1'}[D^{\#}] - k'_{-1'}[D^{\#}] + k'_{1'}[D] \quad (6)$$

$$\frac{d[D]}{dt} = k_1[C^{\#}] + k'_{-1'}[D^{\#}] - k'_{1'}[D] \quad (7)$$

$$\frac{d[C^{\#}]}{dt} = -k_1[C^{\#}] - k'_{-1}[C^{\#}] + k'_1[C] \quad (8)$$

$$\frac{d[C]}{dt} = k_2[AB^{\#}] + k'_{-1}[C^{\#}] - k'_1[C] \quad (9)$$

$$\frac{d[AB^{\#}]}{dt} = -k_2[AB^{\#}] - k'_{-2}[AB^{\#}] + k'_2[A][B] \quad (10)$$

Using steady state approximation, equation 2 can be written as

$$k'_{1'''}[F] - k'_{-1'''}[F^{\#}] - k_{1'''}[F^{\#}] = 0$$

$$[F] = \frac{(k'_{-1'''} + k_{1'''})}{k'_{1'''}}[F^{\#}] \quad (11)$$

From equation (3),

$$k'_{1'''}[E^{\#}] + k'_{-1'''}[F^{\#}] - k'_{1'''}[F] = 0$$

$$k_{1''}[E^{\#}] + k'_{-1'''}[F^{\#}] - k'_{1'''}\frac{(k'_{-1'''} + k_{1'''})}{k'_{1'''}}[F^{\#}] = 0$$

$$[E^{\#}] = \frac{k_{1'''}}{k_{1''}}[F^{\#}] \quad (12)$$

From equation (4),

$$-k_{1''}[E^{\#}] - k'_{-1''}[E^{\#}] + k'_{1''}[E] = 0$$

$$k'_{1''}[E] = (k_{1''} + k'_{-1''})\frac{k_{1'''}}{k_{1''}}[F^{\#}]$$

$$[E] = \frac{k_{1'''}(k_{1''} + k'_{-1''})}{k_{1''}}[F^{\#}] \quad (13)$$

From equation (5),

$$k_{1'}[D^{\#}] + k'_{-1''}[E^{\#}] - k'_{1''}[E] = 0$$

$$k_{1'}[D^{\#}] + k'_{-1''}\left(\frac{k_{1'''}}{k}\right)[F^{\#}] - \frac{k_{1'''}(k_{1''} + k'_{-1''})}{k_{1''}}[F^{\#}] = 0$$

$$[D^{\#}] = \frac{k_{1'''}}{k_{1'}}[F^{\#}] \quad (14)$$

From equation (6),

$$-k_{1'}[D^{\#}] - k'_{-1''}[D^{\#}] + k'_{1'}[D] = 0$$

$$[D] = \frac{k_{1'''}(k_{1'} + k'_{1'})}{k_{1'}k'_{1'}}[F^{\#}] \quad (15)$$

From equation (7),

$$k_1[C^{\#}] + k'_{-1'}[D^{\#}] - k'_{1'}[D] = 0$$

$$k_1[C^{\#}] + k'_{-1'}\frac{k_{1'''}}{k_{1'}}[F^{\#}] - \frac{k_{1'''}(k_{1''} + k'_{1'})}{k_{1'}}[F^{\#}] = 0$$

$$[C^{\#}] = \frac{k_{1'''}k'_{1'}}{k_1k_{1'}}[F^{\#}] \quad (16)$$

From equation (8),

$$-k_1[C^{\#}] - k'_{-1}[C^{\#}] + k'_1[C] = 0$$

$$k'_1[C] = (k_1 + k'_{-1})[C^{\#}] = \frac{k_{1'''}k'_{1'}(k_1 + k'_{-1})}{k_1k_{1'}}[F^{\#}]$$

$$[C] = \frac{k_{1'''}k'_{1'}(k_1 + k'_{-1})}{k_1k_{1'}k'_1}[F^{\#}] \quad (17)$$

From equation (9),

$$k_2[AB^{\#}] + k'_{-1}[C^{\#}] - k'_1[C] = 0$$

$$k_2[AB^{\#}] + k'_{-1}\left(\frac{k_{1'''}k'_{1'}}{k_1k_{1'}}\right)[F^{\#}] - k'_1\left(\frac{k_{1'''}k'_{1'}(k_1 + k'_{-1})}{k_1k_{1'}k'_1}\right)[F^{\#}] = 0$$

$$[AB^{\#}] = \frac{k_{1'''}k'_{1'}}{k_2k_{1'}}[F^{\#}] \quad (18)$$

From equation (10),

$$-k_2[AB^{\#}] - k'_{-2}[AB^{\#}] + k'_2[A][B] = 0$$

$$(k_2 + k'_{-2})[AB^{\#}] = k'_2[A][B]$$

$$k'_2[A][B] = (k_2 + k'_{-2})\left(\frac{k_{1'''}k'_{1'}}{k_2k_{1'}}\right)[F^{\#}]$$

$$[F^{\#}] = \frac{k_2k'_2k_{2'}}{k_{2'''}k'_{2'}(k_2 + k'_{-2})}[A][B] \quad (19)$$

Therefore using equation (19) equation (1) can be written thus;

$$\frac{d[P]}{dt} = \frac{k_2k'_2k_{1'}}{k'_{1'}(k_2 + k'_{-2})}[A][B] \quad (20)$$

where $\frac{k_2k'_2k_{1'}}{k'_{1'}(k_2 + k'_{-2})} = K$, the experimental rate constant.

CONCLUSION

The formation of 5-(4-methoxyphenyl)-1,3,4-oxadiazol-2-amine through cyclization of (E)-2-(4-methoxybenzylidene)hydrazinecarboxamide has been investigated using semi-empirical/Austin model (AM1) and Density functional theory (DFT) [RB3LYP/6-31G(d)] calculations in SPARTAN,2009 program suit. The two reaction path ways were found to consist several elementary steps comprising intermediate and transition states. The cyclization of (E)-2-(4-methoxybenzylidene)hydrazinecarboxamide was found via two routes. From the kinetic data it was observed that the consecutive step between second and third intermediates with rate constant value of 1.64 s^{-1} is the rate determining step and the overall rate for the first reaction mechanism. But for the alternative reaction pathway, the step between the third and fourth intermediates with rate constant value of 1.44×10^{-4} s^{-1} is the rate determining step. Though two cyclization routes were all endothermic, cyclization route 2 was more endothermic. Hence, the reaction path way (route 1) was most stable favorable as shown in the potential energy curve. This is also collaborated by the thermodynamic data for the two reaction pathways. 5-(4-methoxyphenyl)-1,3,4-oxadiazol-2-amine formation mechanism has high energy demand typical of cyclization reaction.

REFERENCES

1. J. F. Dorgan, J. W. Brock, N. Rothman, L. L. Needham, R. Miller, H. E. Stephenson Jr, N. Schussler -and P. R. Taylor, *Cancer Causes Contr*., **1999**, *10*, 1.
2. (a) M. Amir and S. Shahani, *Indian J. Heterocycl. Chem*., **1998,** *8*, 107; (b) F. A. Omar, N. M. Mahfouz and M. A. Rahman, *Eur. J. Med. Chem*., **1996,** *31***,** 819; (c) M. Kidwai, N. Negi and S.R. Chowdhury, *Acta Pharmaceutica,* **1995**, *45*, 511; (d) M. Amir and R. Agarwal, *Indian J. of Heterocycl. Chem.*, **1998,** *7,* 225.
3. (a) F. A. Ashour and S. A. Al Mazoroa, *J. Pharm. Sci.*, **1990,** *4*, 29; (b) I. A. Shehata, M. N. Nasr, H. I. El Subbagh, M. M.

Gineinah and S. M. Kheira, *Scientia Pharmaceutic*., **1996,** *64*, 133.
4. (a) O. M. Nassar, *Indian J. Heterocycl. Chem*., **1997,** *7,* 105; (b) P. Tsitsa, A. P. Valiraki, T. S. Papastaikoudi, Z. P. Daifoiti, and A. Vamvakidis, *Ann Pharm Fr*., **1989,** *47,* 296.
5. N. A. Mohamed, *Polymer. Degrad. and Stab.,* **1994,** *44,* 33.
6. H. L. Plant, R. R. Regis and R. C. Moore, Eur. Pat. Appl. EP 156638 A2, 1985.
7. I. R. Matthews and D. P. Bacon, PCT Int. Appl. WO 9505368 A1, 1995.
8. U. Kraatz, B. Gallenkamp, A. Marhold and P. Wolfrum, WO 2002006256 A1, 2002.
9. J. P. Arrington and L. L. Wade, US Patent 42, 151, 29 1980.
10. M. Singhal and A. Paul, *Res. J. Pharm.,* **2011,** *5*, 47.
11. K. Sriram, S. A. Benkovic, M. A. Hebert, D.B. Miller and J. P. O'Callaghan, *J. Bio. Chem*., **2004,** *79,* 19936.d
12. (a) A. D. Becke, *J. Chem. Phys*., **1993,** 98, 5648; (b) C. Lee, W. Yang and R. G. Parr, *Condens. Matter Mater. Phys.*, **1988,** *37,* 785.
13. C. Gonzalez and H. B. Schlegel, *J. Phys. Chem*., **1989,** *90*, 2154.
14. E. Thomas and R. Philip, "Physical Chemistry", Rev. Ed. Pearson: Washington, USA, 2006.